Synthesis of silicone elastomers containing trifluoropropyl groups and their use in dielectric elastomer transducers

Mihaela Dascalu,[a†] Simon J. Dünki,[a,b] Jose-Enrico Q. Quinsaat,[a,b] Yee Song Ko,[a,b] Dorina M. Opris[a*]

[a] *Empa, Swiss Federal Laboratories for Materials Science and Technology, Laboratory for Functional Polymers, Ueberlandstr. 129, CH-8600, Dübendorf, Switzerland, E-mail: dorina.opris@empa.ch.*

[b] *Ecole Polytechnique Fédérale de Lausanne (EPFL), Institut des matériaux, Station 12, CH 1015, Lausanne, Switzerland.*

† *Present address: Petru Poni Institute of Macromolecular Chemistry, Aleea Grigore Ghica Voda 41A, Iasi, 700487, Romania*

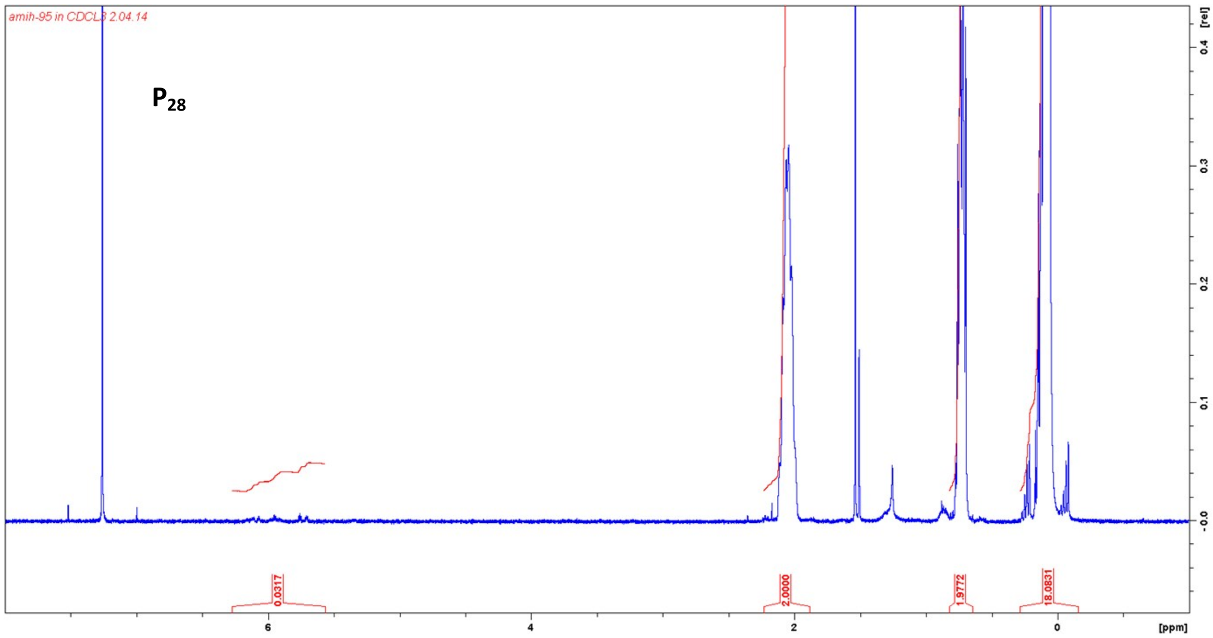

Fig. S1 ^{1}H NMR spectrum of $\mathbf{P_{28}}$ in $CDCl_3$ at room temperature.

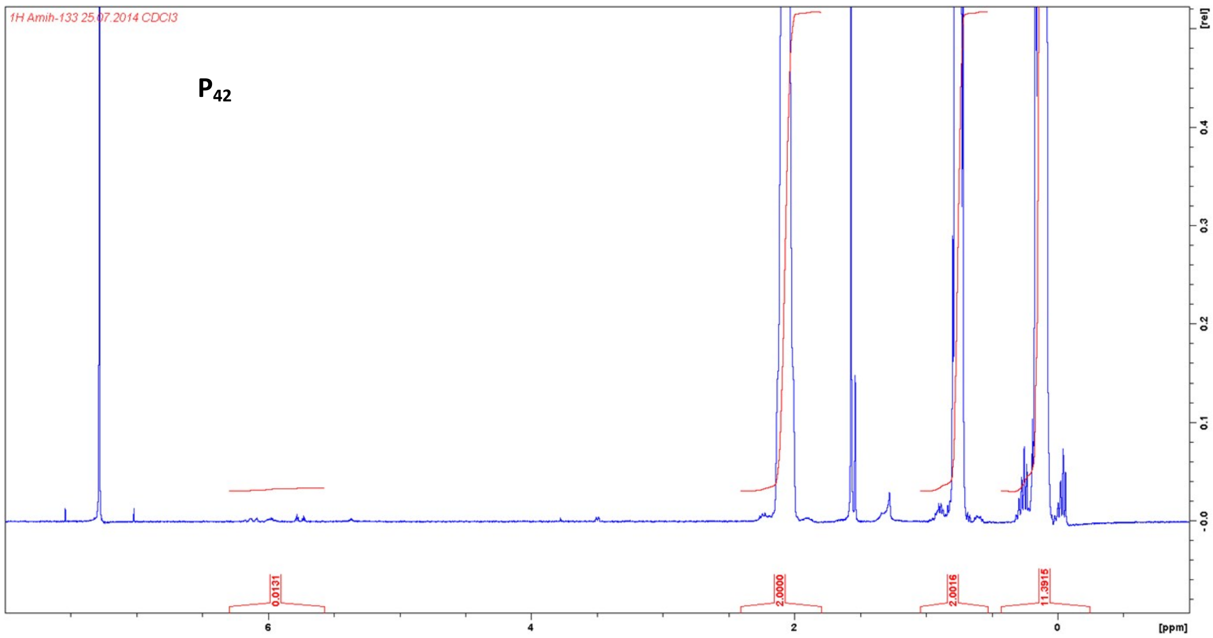

Fig. S2 ^{1}H NMR spectrum of $\mathbf{P_{42}}$ in $CDCl_3$ at room temperature.

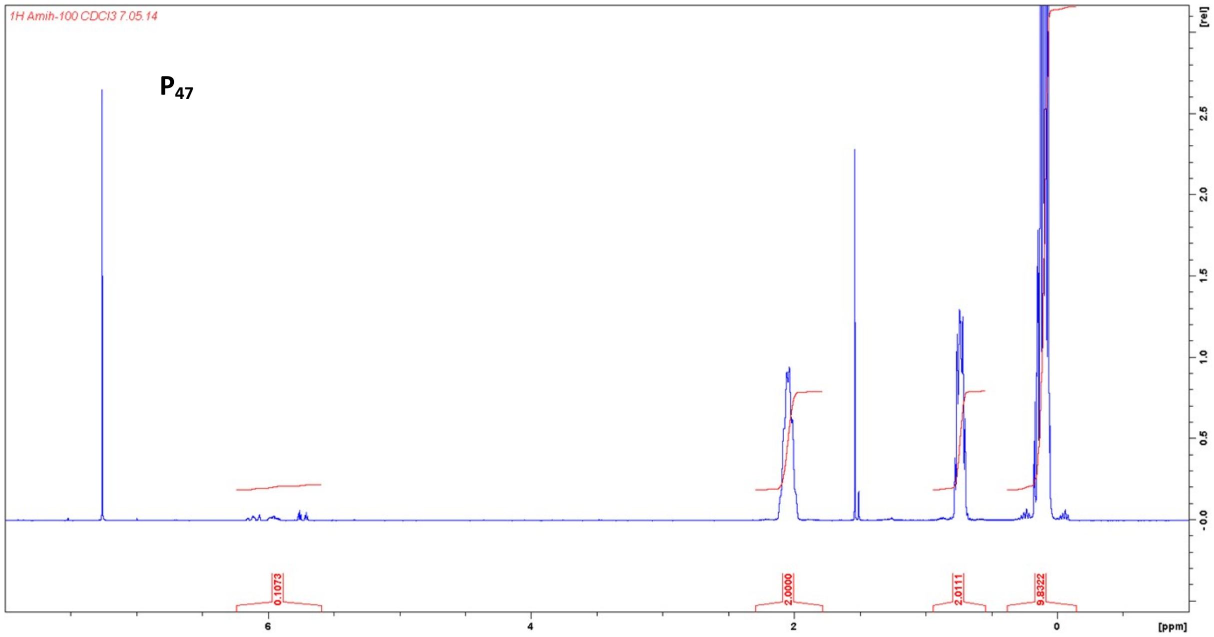

Fig. S3 ^{1}H NMR spectrum of $\mathbf{P_{47}}$ in $CDCl_3$ at room temperature.

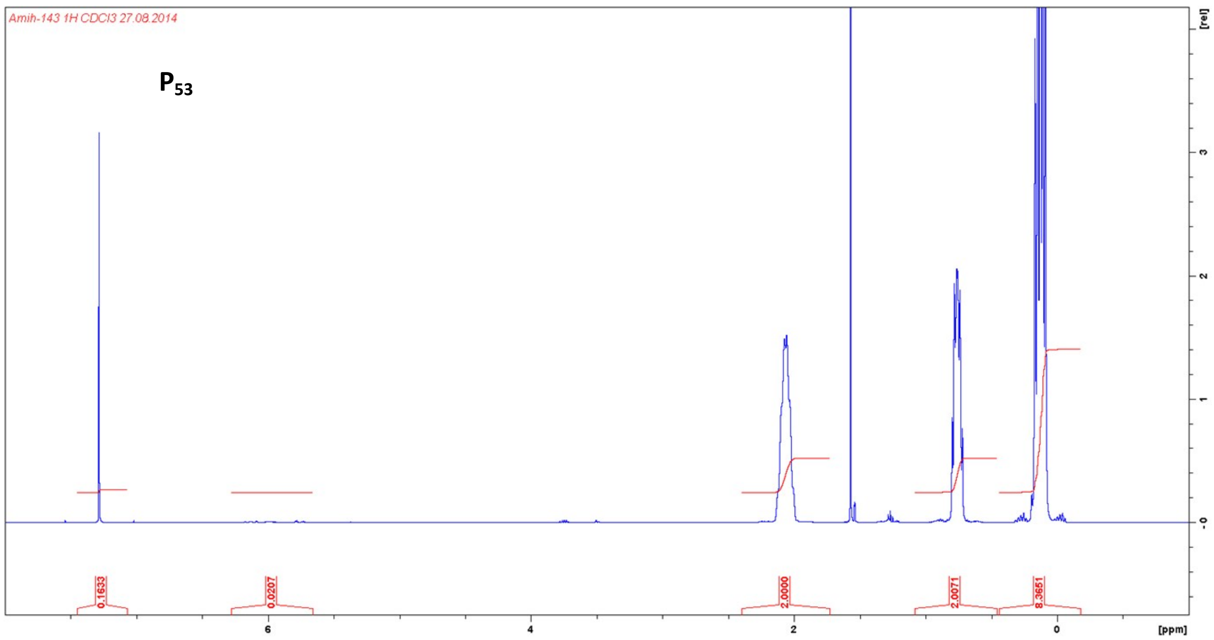

Fig. S4 ^{1}H NMR spectrum of $\mathbf{P_{53}}$ in $CDCl_3$ at room temperature.

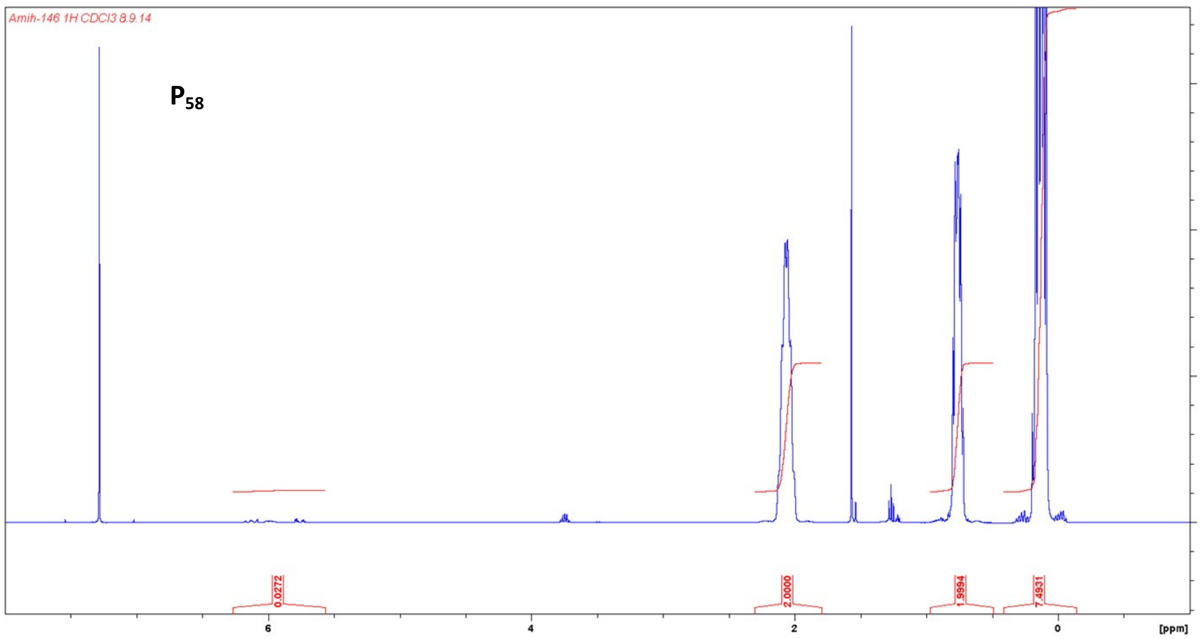

Fig. S5 ^{1}H NMR spectrum of $\mathbf{P_{58}}$ in $CDCl_3$ at room temperature.

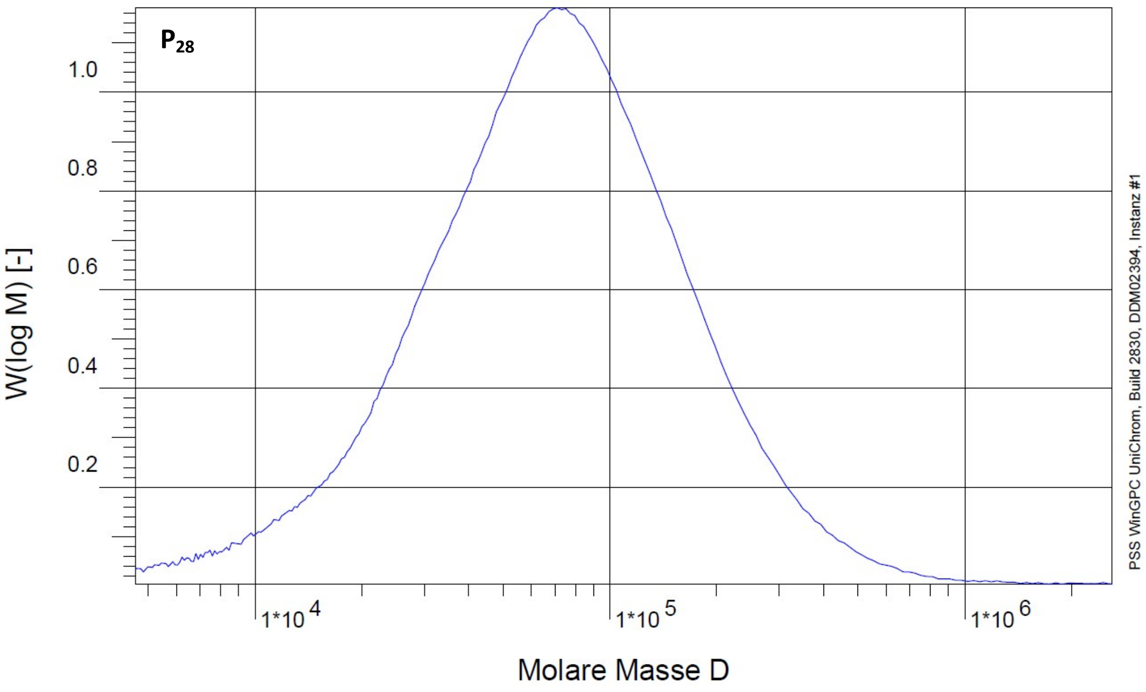

Mn :	4.6762e4	g/mol
Mw :	1.0172e5	g/mol
Mz :	2.5320e5	g/mol
Mv :	0.000000	g/mol
D :	2.1754e0	

Fig. S6 GPC of $\mathbf{P_{28}}$ in THF.

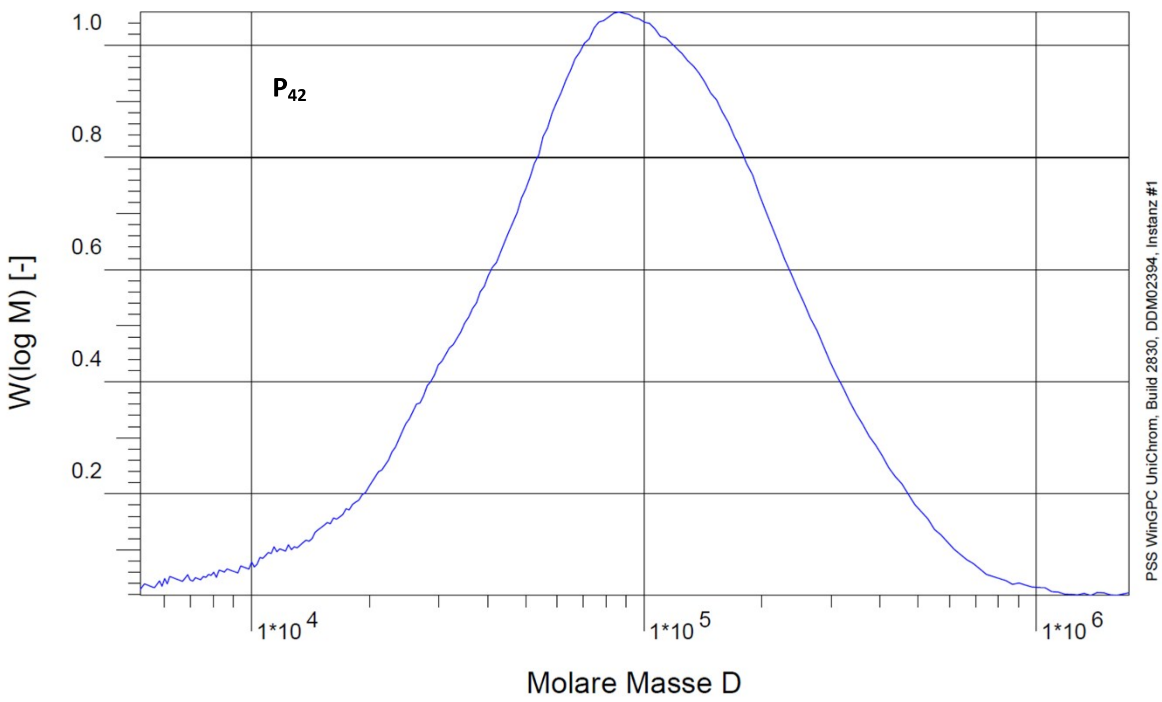

Mn :	5.9191e4	g/mol
Mw :	1.4017e5	g/mol
Mz :	3.1178e5	g/mol
Mv :	0.000000	g/mol
D :	2.3681e0	

Fig. S7 GPC of **P_{42}** in THF.

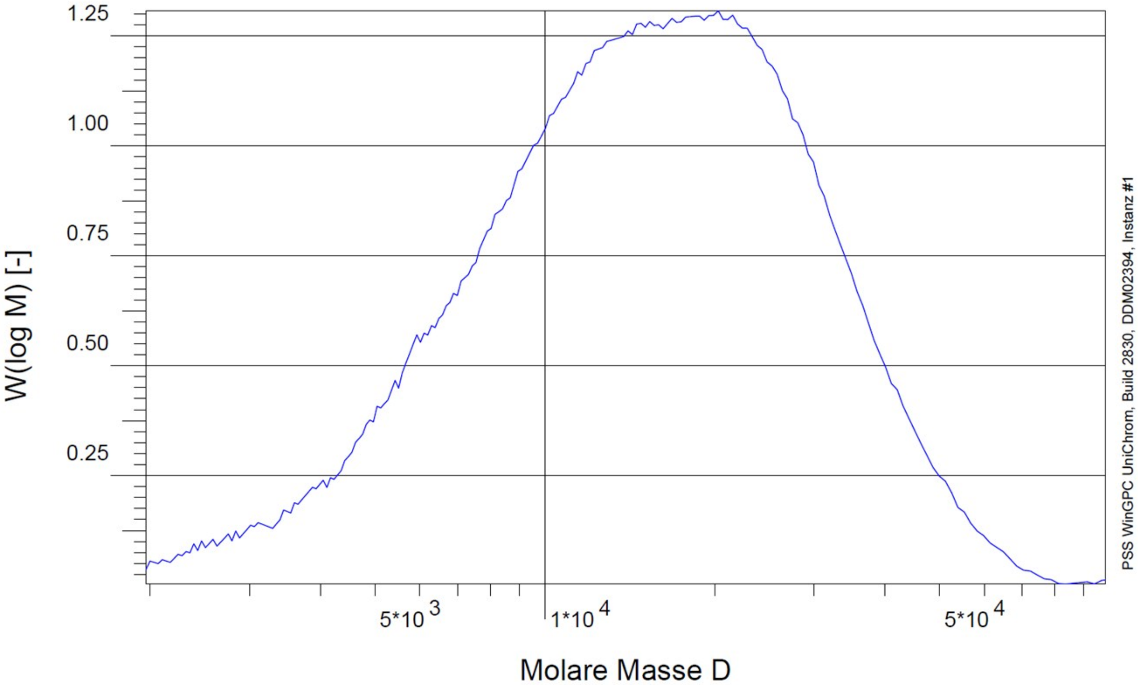

Mn :	1.1599e4	g/mol
Mw :	1.8191e4	g/mol
Mz :	2.5863e4	g/mol
Mv :	0.000000	g/mol
D :	1.5683e0	

Fig. S8 GPC of $\mathbf{P_{47}}$ in THF.

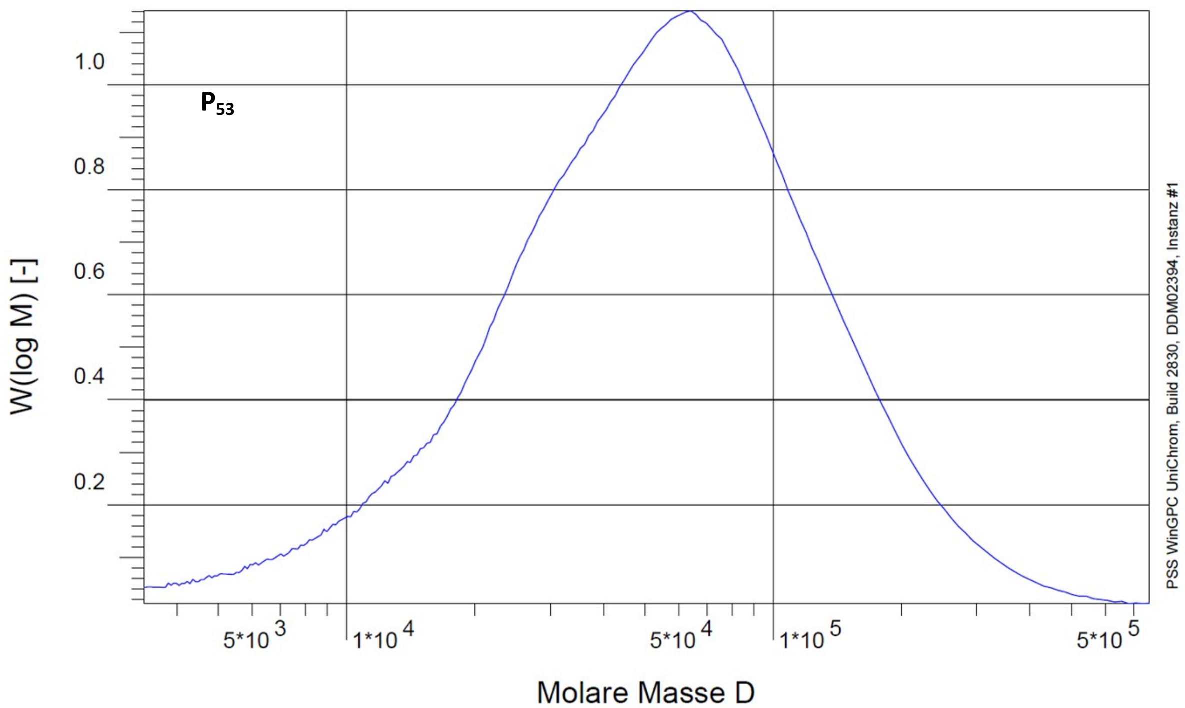

Mn :	3.4709e4	g/mol
Mw :	7.5884e4	g/mol
Mz :	1.4513e5	g/mol
Mv :	0.000000	g/mol
D :	2.1863e0	

Fig. S9 GPC of $\mathbf{P_{53}}$ in THF.

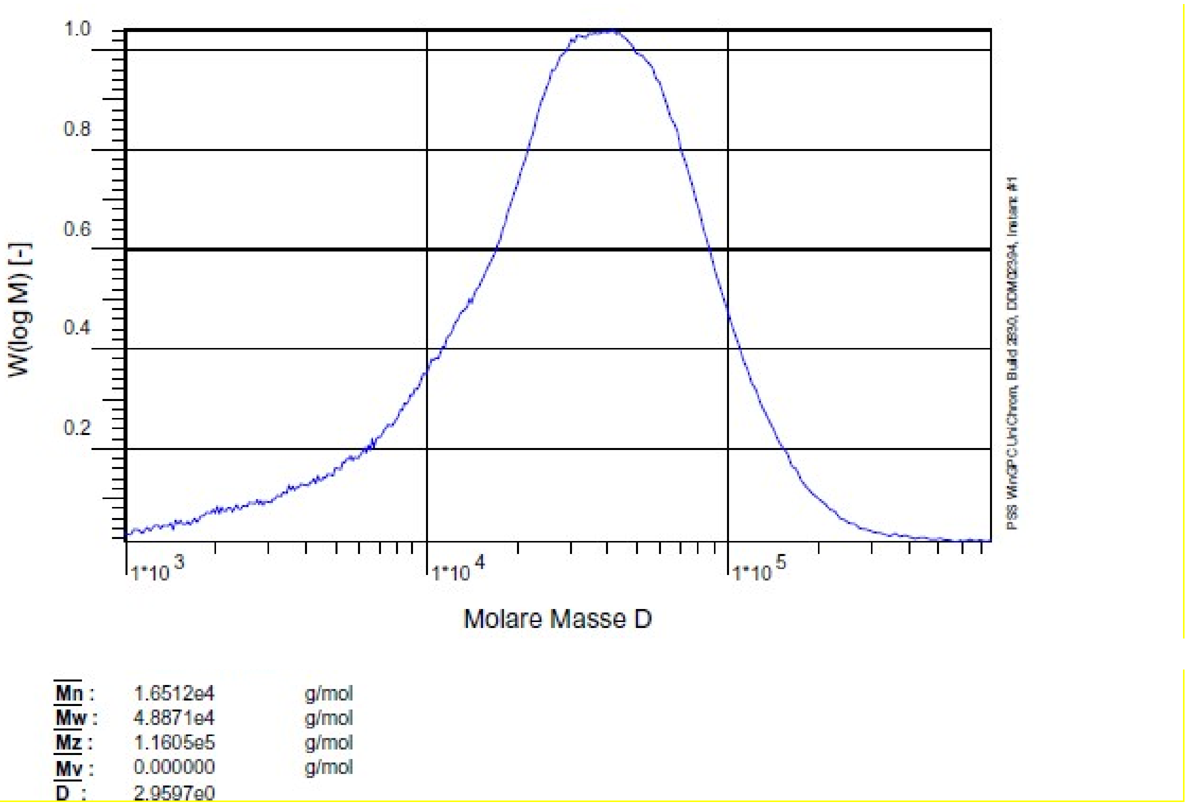

Fig. S10 GPC of $\mathbf{P_{58}}$ in THF.

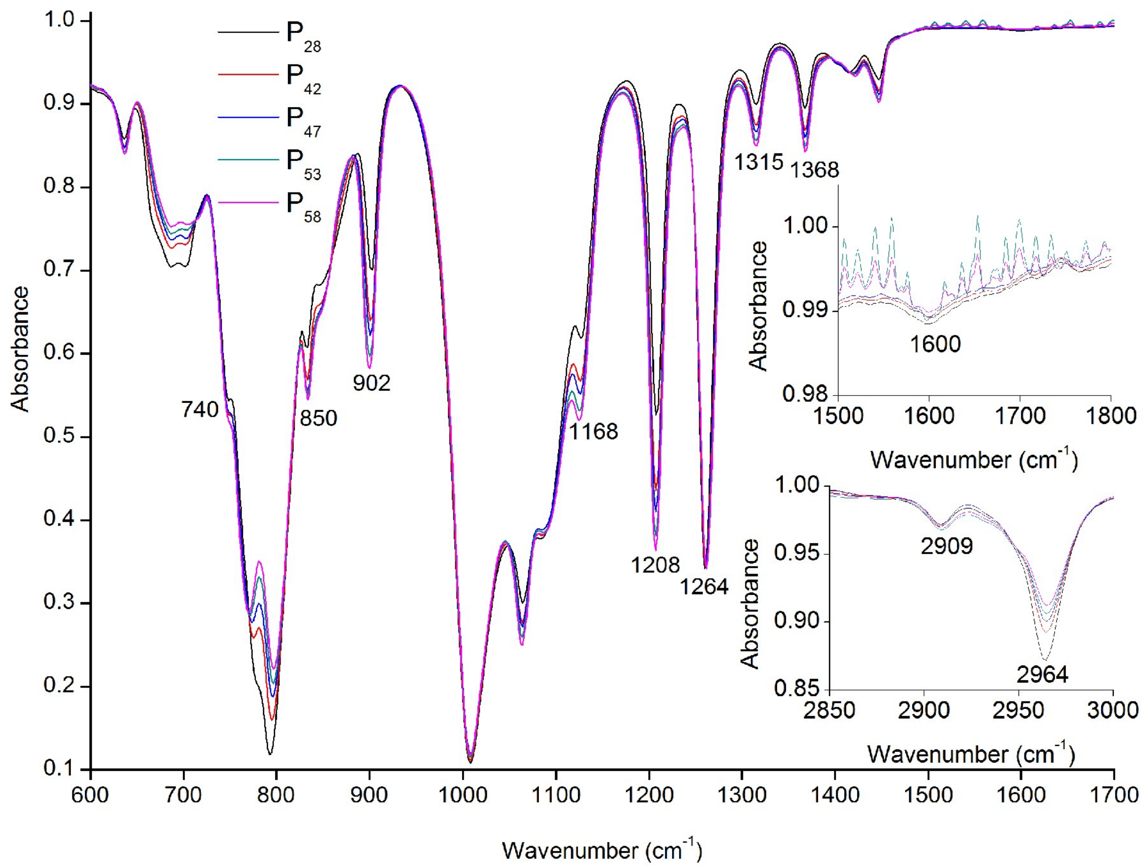

Fig. S11 FTIR spectra of $\mathbf{P_x}$.

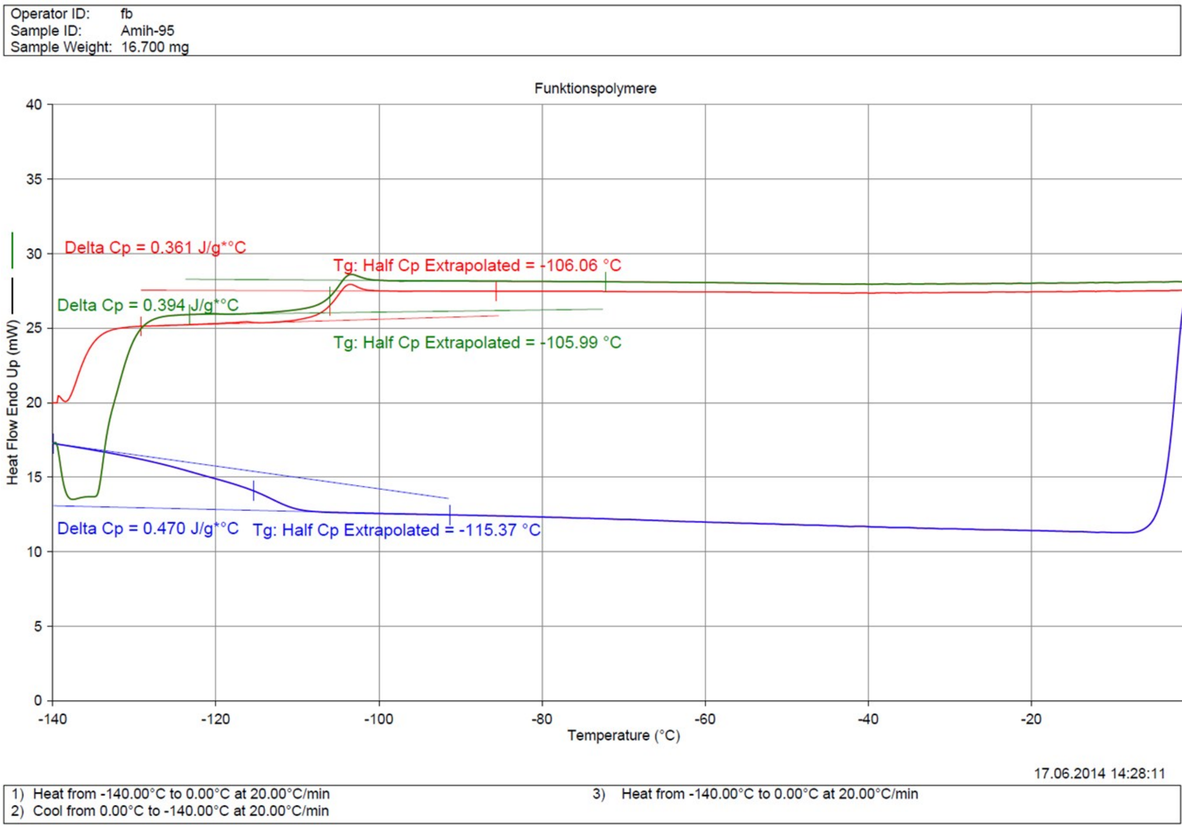

Fig. S12 DSC curves of $\mathbf{P_{28}}$.

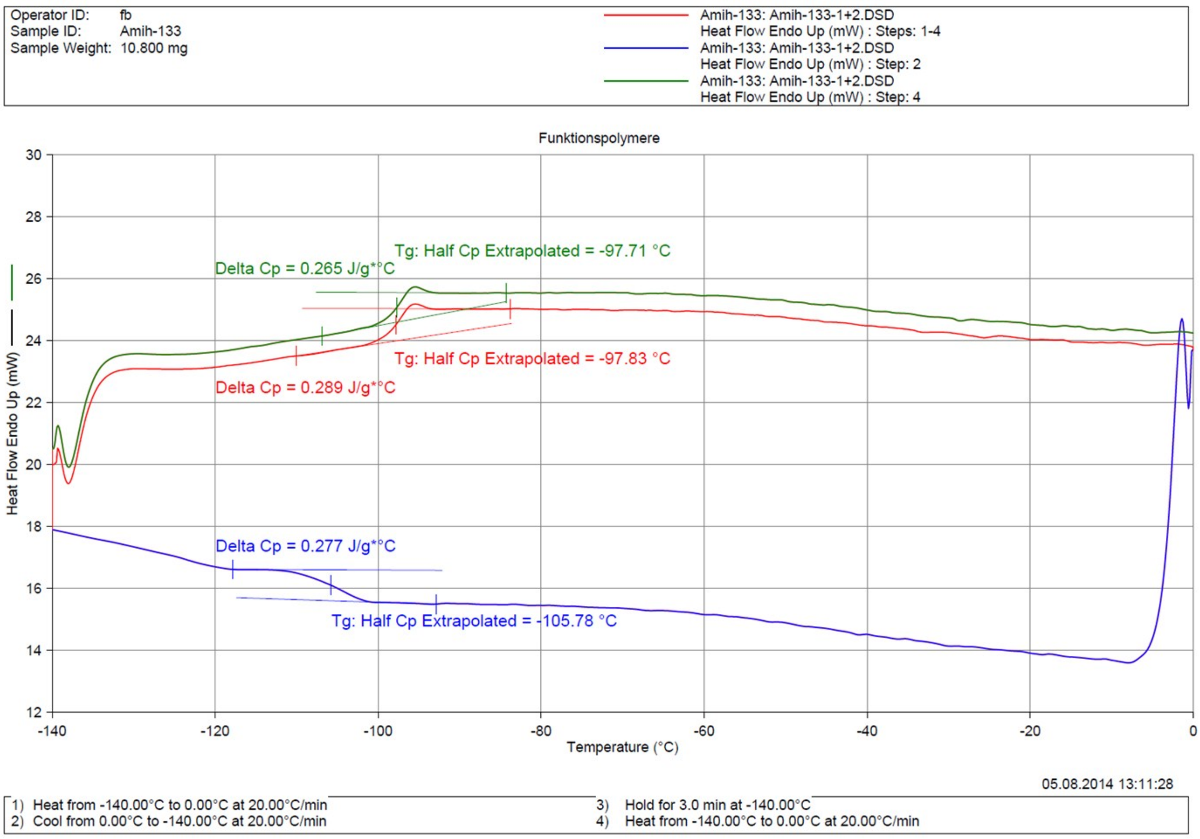

Fig. S13 DSC curves of P_{42}.

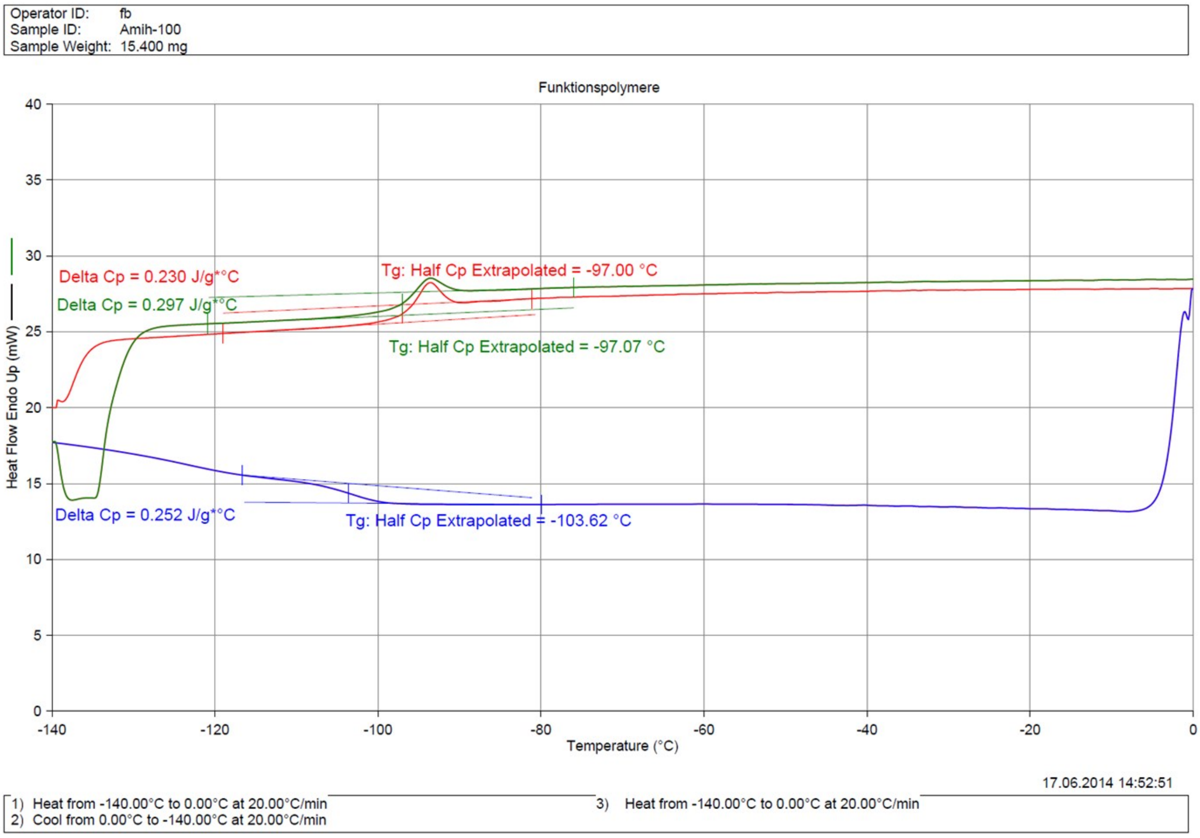

Fig. S14 DSC curves of $\mathbf{P_{47}}$.

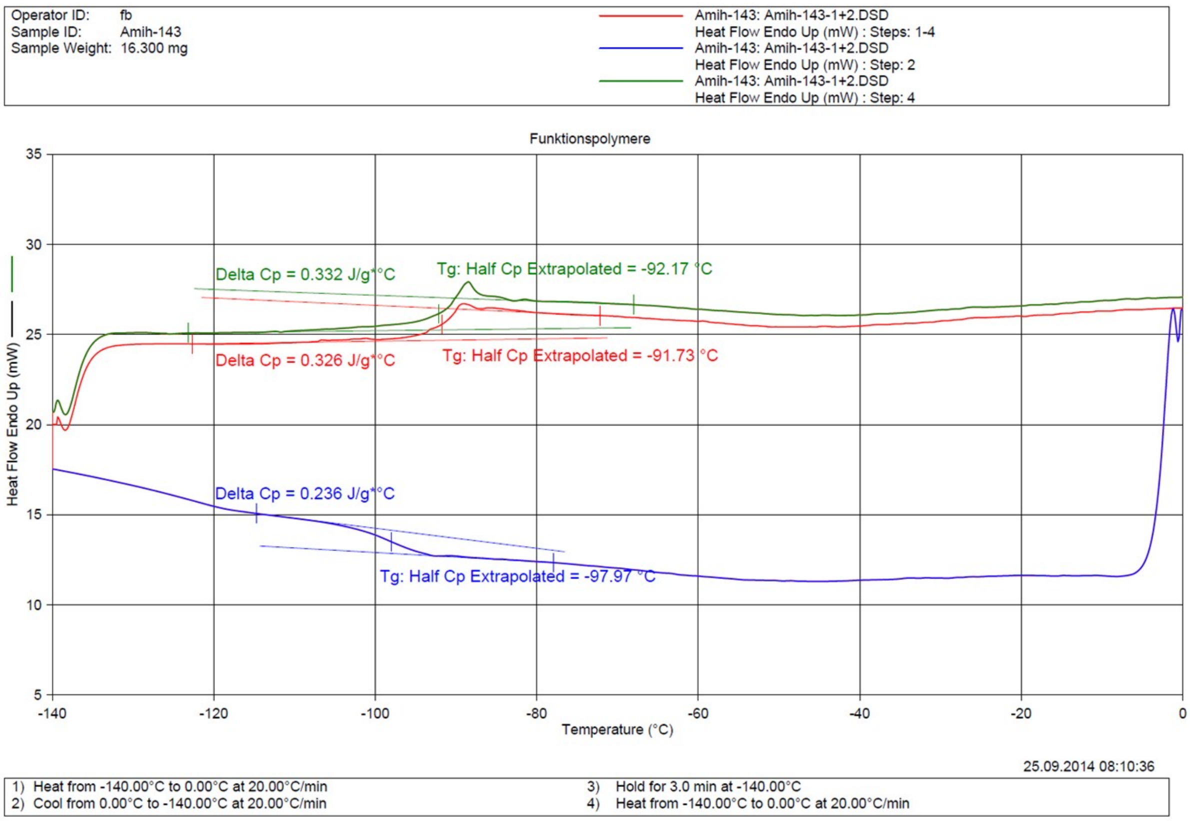

Fig. S15 DSC curves of $\mathbf{P_{53}}$.

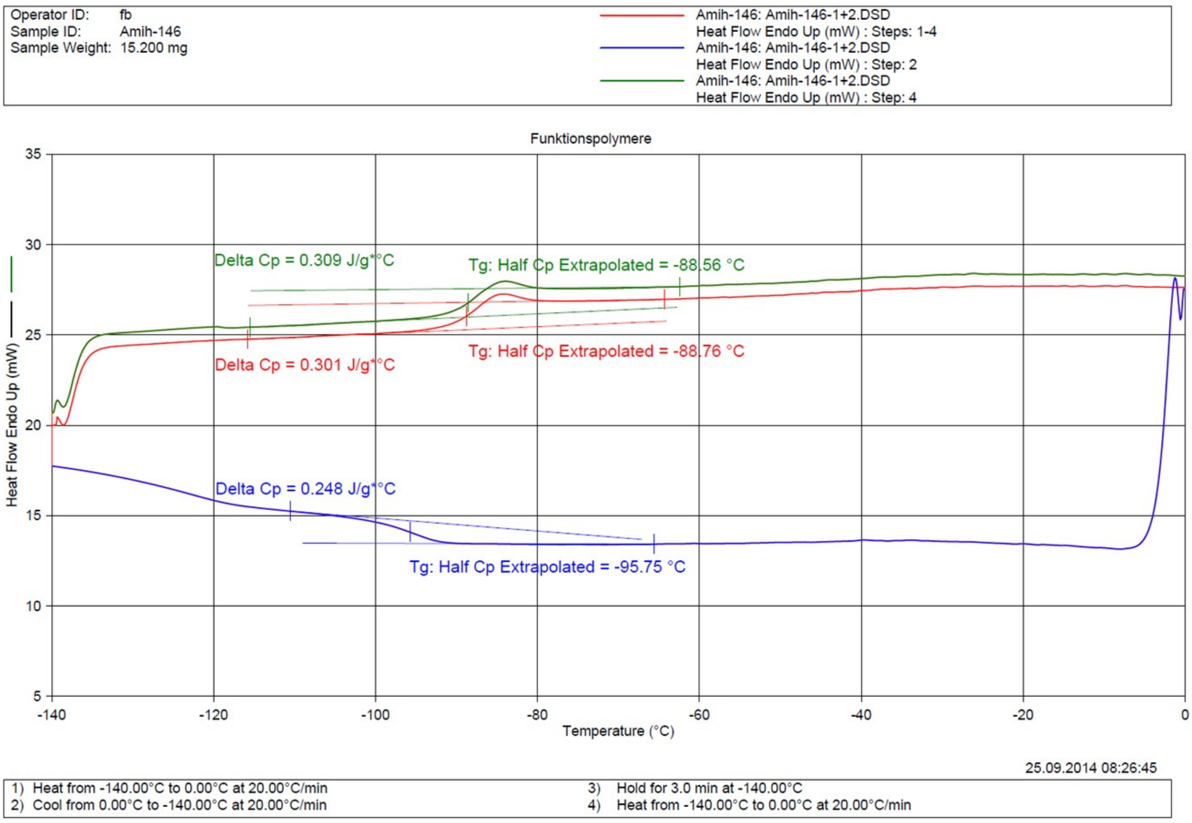

Fig. S16 DSC curves of $\mathbf{P_{58}}$.

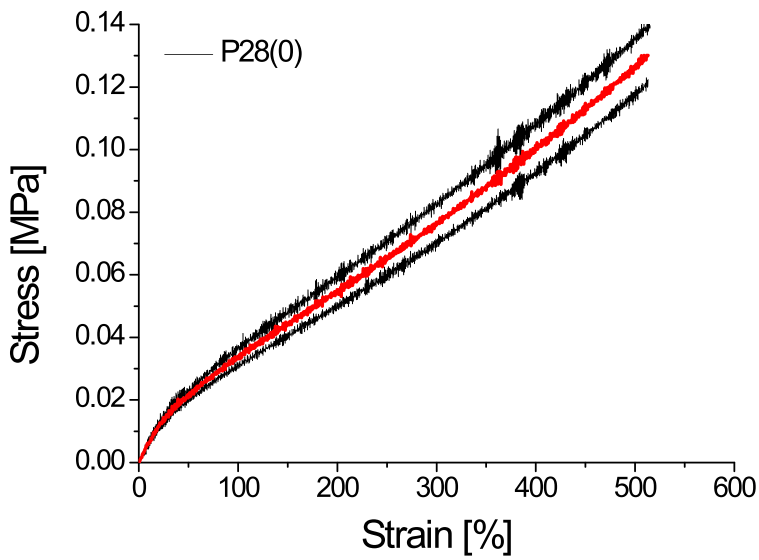

Fig. S17 Stress-strain curves of material $\mathbf{P_{28}(0)}$. The red curve represents the average.

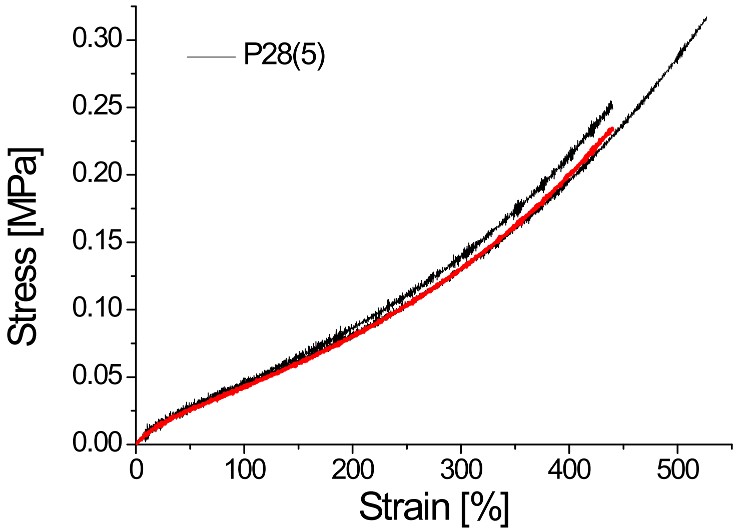

Fig. S18 Stress-strain curves of material **P_{28}(5)**. The red curve represents the average.

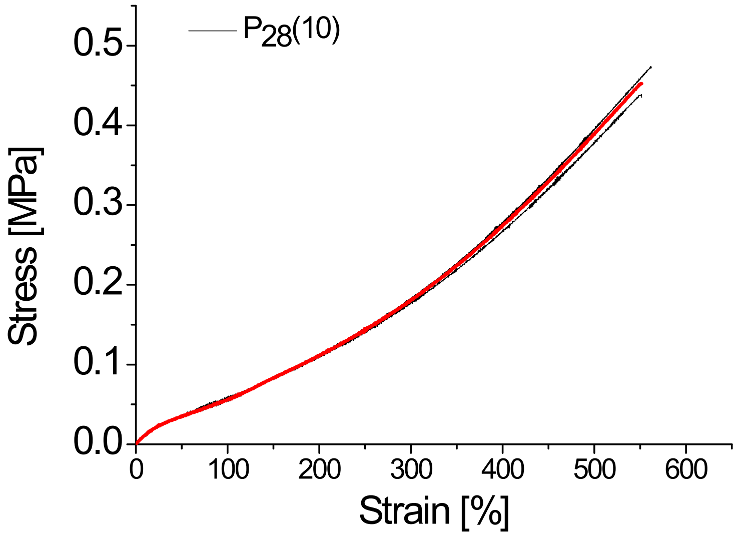

Fig. S19 Stress-strain curves of material **P_{28}(10)**. The red curve represents the average.

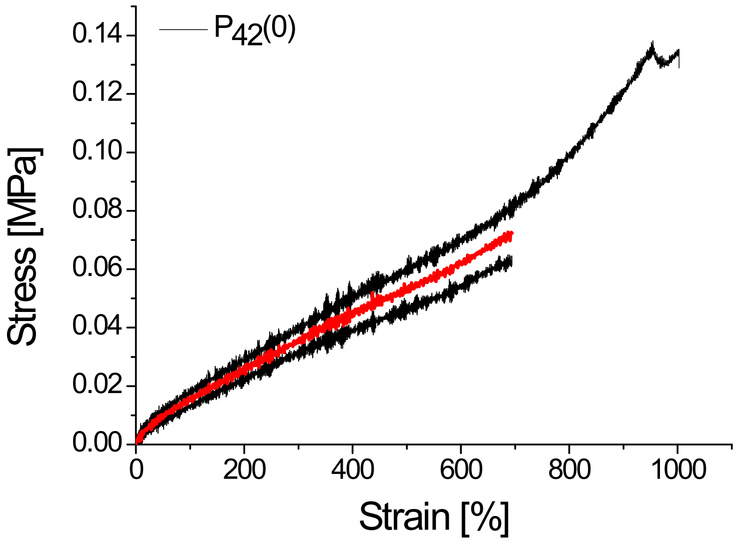

Fig. S20 Stress-strain curves of material $\mathbf{P_{42}(0)}$. The red curve represents the average.

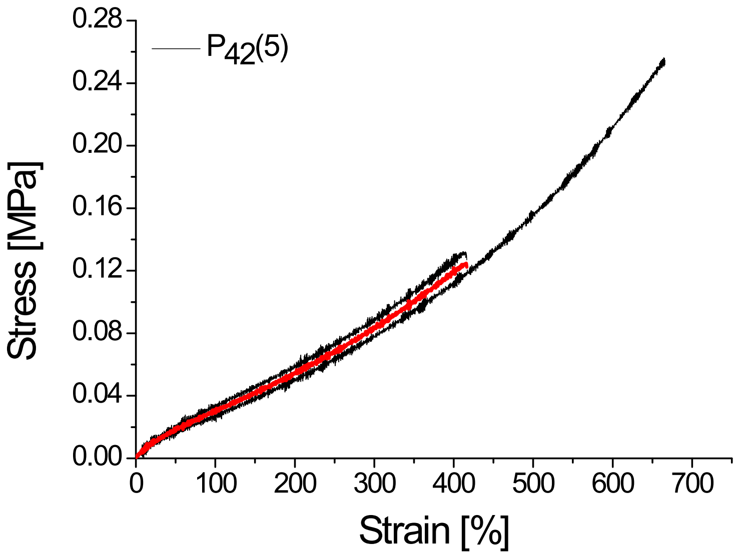

Fig. S21 Stress-strain curves of material $\mathbf{P_{42}(5)}$. The red curve represents the average.

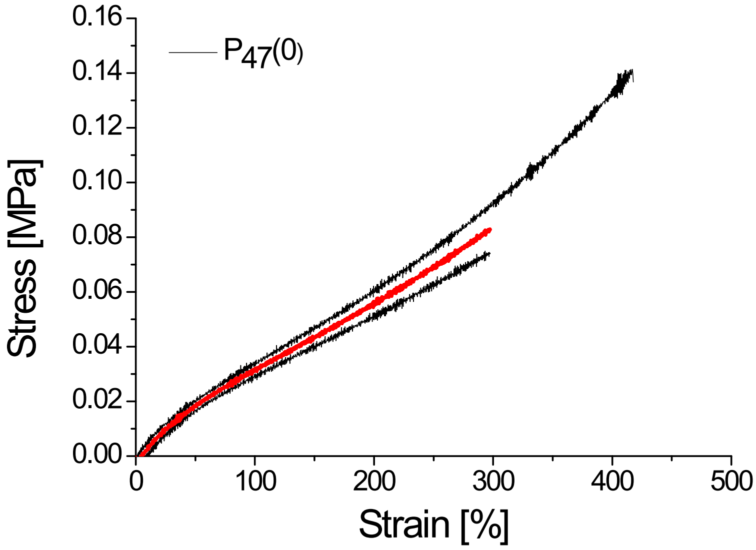

Fig. S22 Stress-strain curves of material $\mathbf{P_{47}(0)}$. The red curve represents the average.

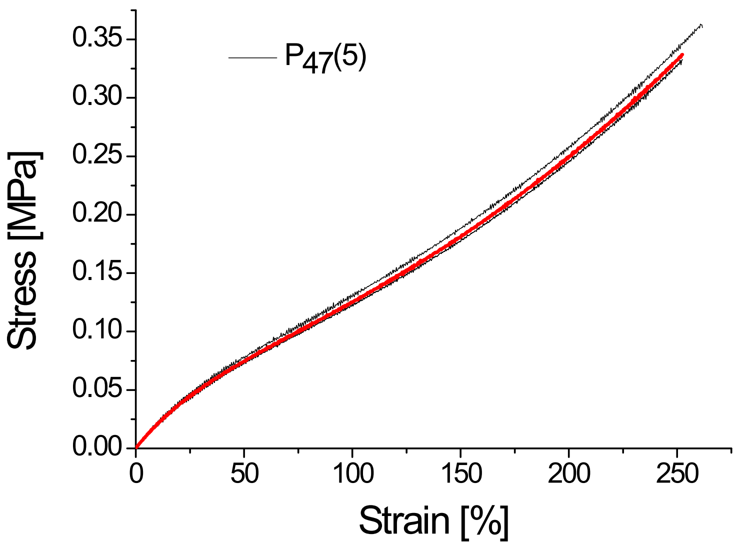

Fig. S23 Stress-strain curves of material $\mathbf{P_{47}(5)}$. The red curve represents the average.

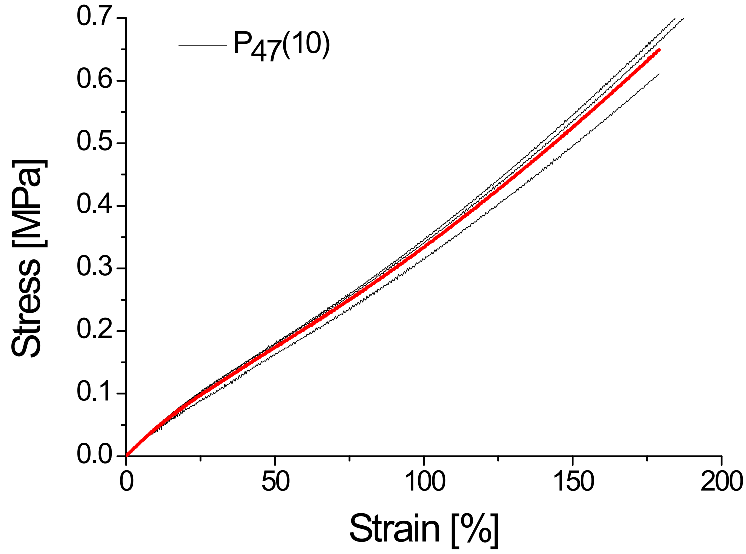

Fig. S24 Stress-strain curves of material $\mathbf{P_{47}(10)}$. The red curve represents the average.

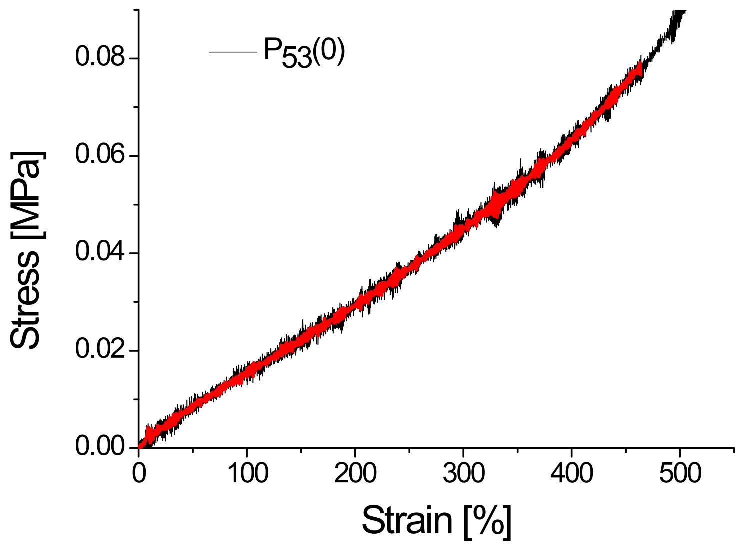

Fig. S25 Stress-strain curves of material $\mathbf{P_{53}(0)}$. The red curve represents the average.

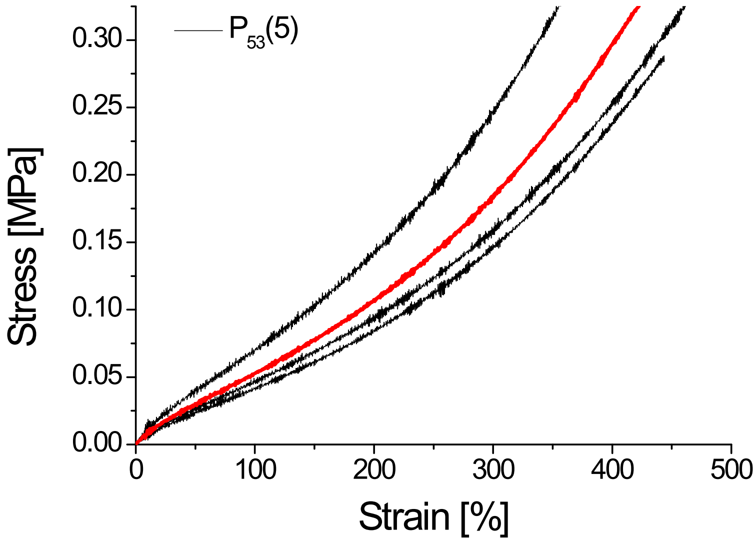

Fig. S26 Stress-strain curves of material **P_{53}(5)**. The red curve represents the average.

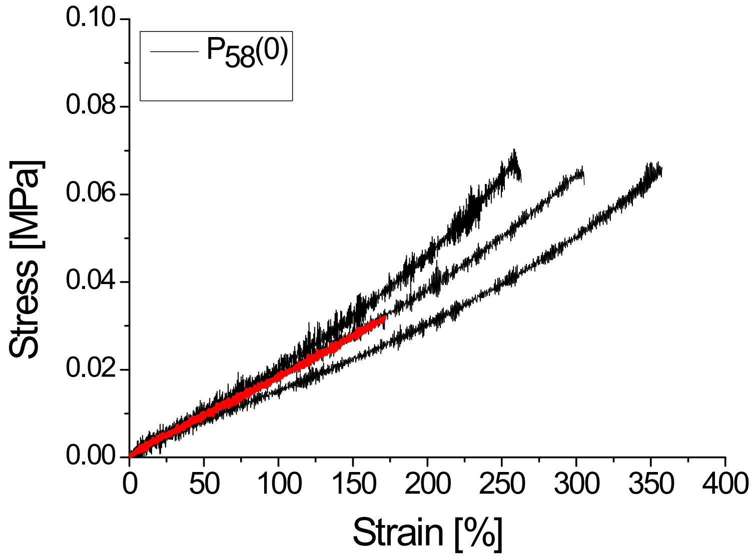

Fig. S27 Stress-strain curves of material **P_{58}(0)**. The red curve represents the average.

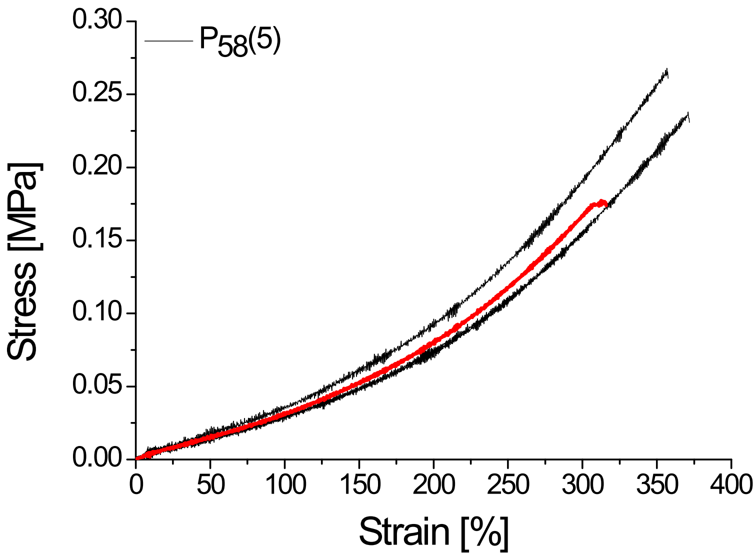

Fig. S28 Stress-strain curves of material **P_{58}(5)**. The red curve represents the average.

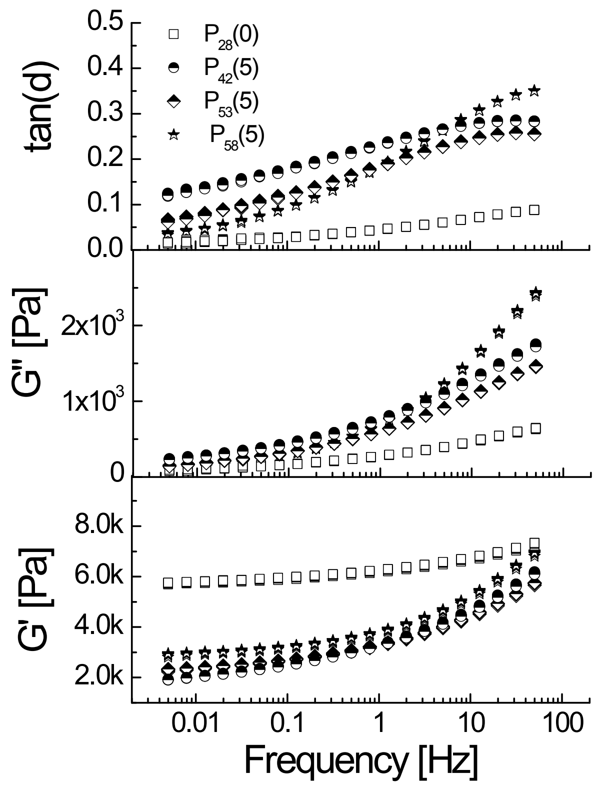

Fig. 29 Dependence of the real (G') and imaginary (G'') parts of the shear modulus and the tan(d) at room temperature for selected materials. The samples used had a thickness of 263 μm - **P_{58}(5)**, 180 μm –**P_{53}(5)**, 187 μm - **P_{42}(5)**, **P_{28}(0)** – 250 μm and were measured one year after their synthesis.

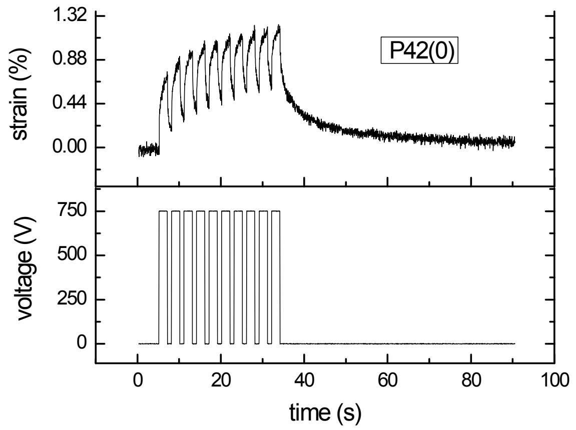

Fig. S30 Cyclic actuation tests of $\mathbf{P_{42}(0)}$ at 4.3 V/μm (10 cycles at 0.33 Hz).

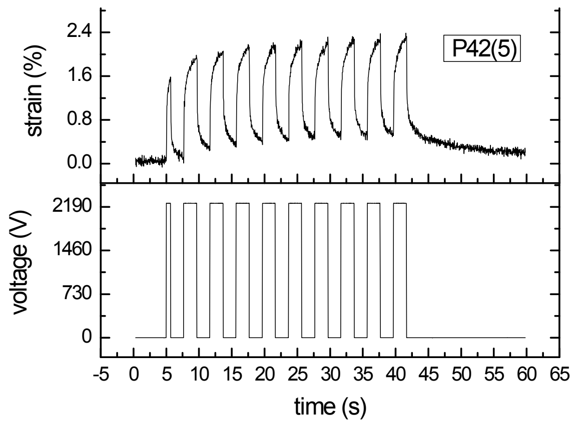

Fig. S31 Cyclic actuation strain of $\mathbf{P_{42}(5)}$ at 7.1 V/μm (10 cycles at 0.25 Hz).

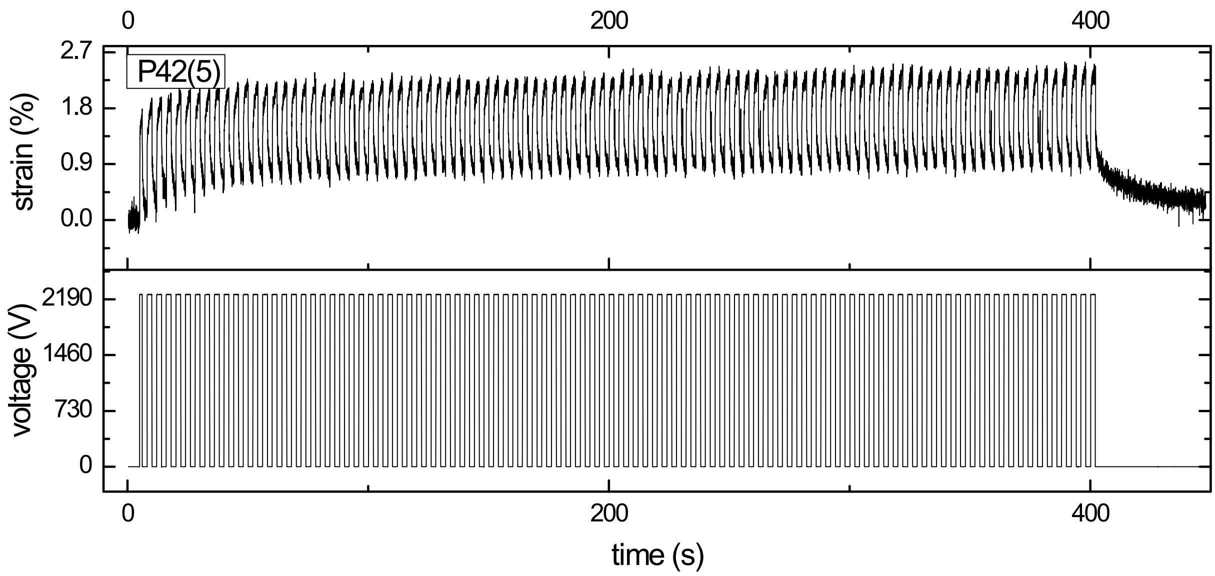

Fig. S32 Cyclic actuation strain of $\mathbf{P_{42}(5)}$ at 7.1 V/μm (100 cycles at 0.25 Hz).

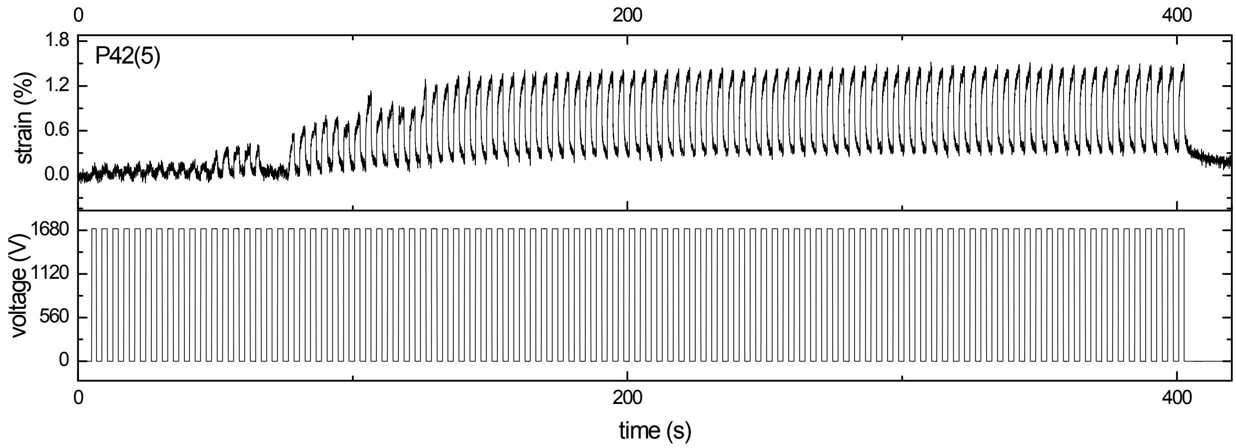

Fig. S33 An actuator constructed from $\mathbf{P_{42}(5)}$ which suffered a shortcut and can self-repair after few cycles at 5.5 V/μm and 0.25 Hz.

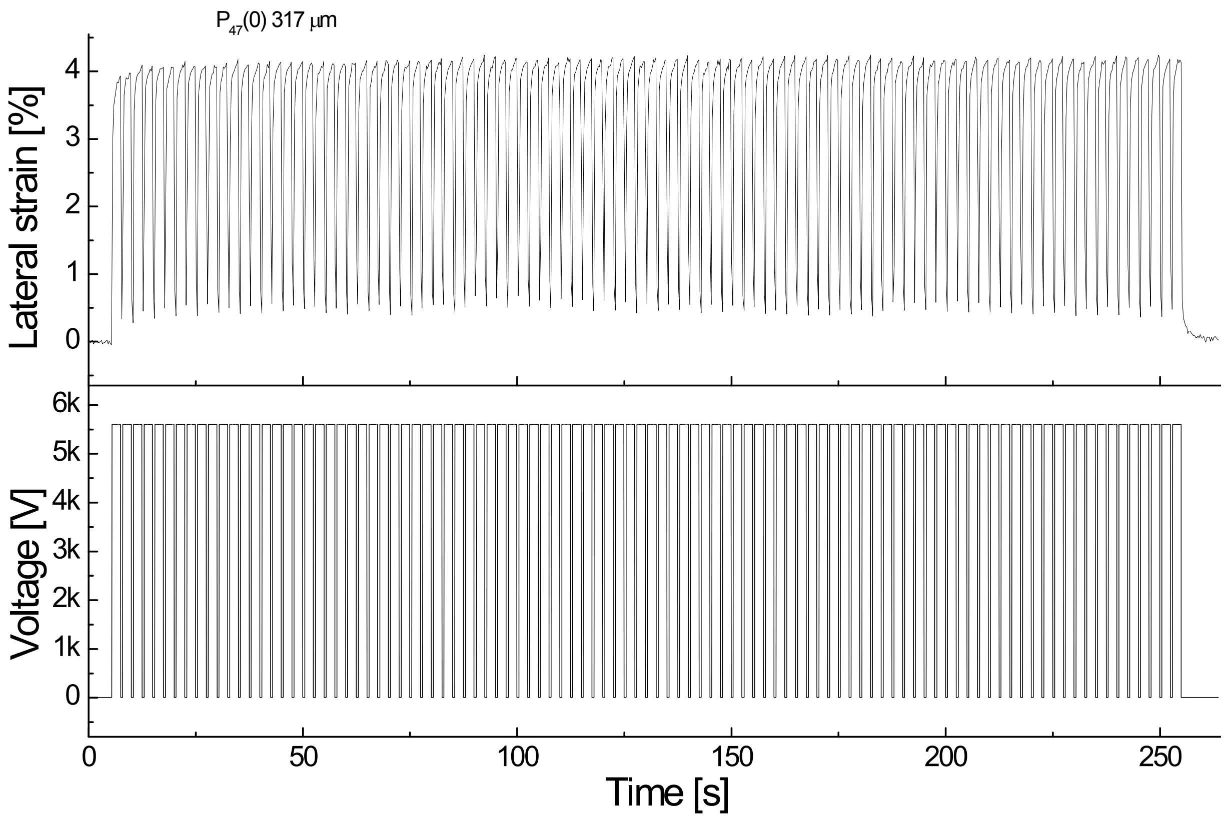

Fig. S34 Cyclic actuation strain of $\mathbf{P_{47}(0)}$ at 17.6 V/μm (100 cycles at 0.4 Hz).

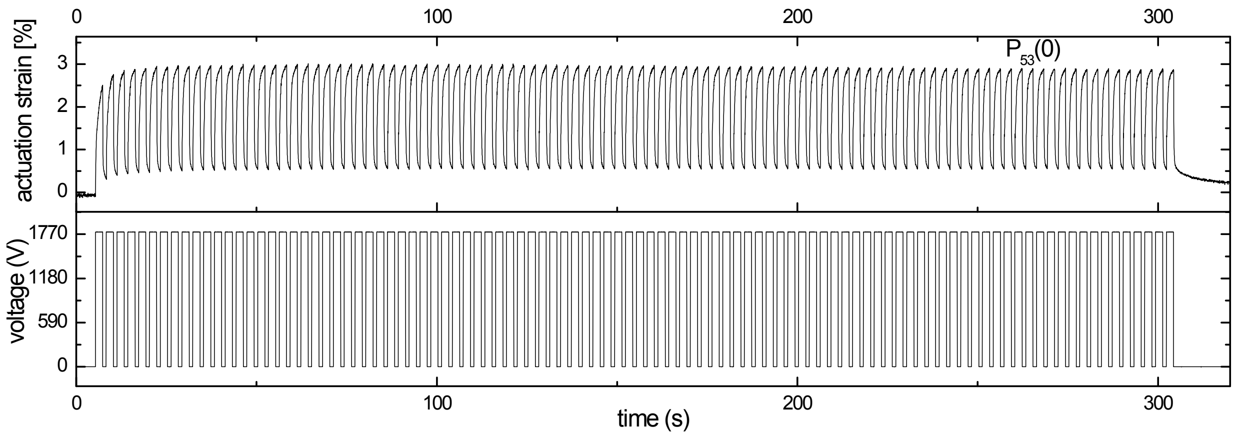

Fig. S35 Cyclic actuation strain of **P_{53}(0)** at 5.6 V/μm (100 cycles at 0.33 Hz).

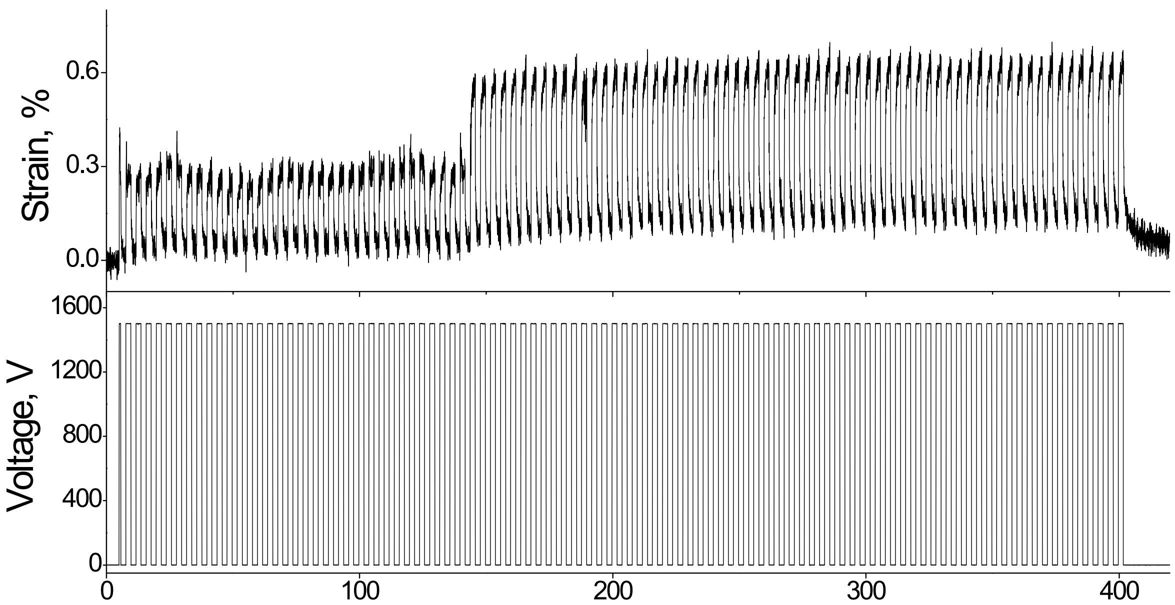

Fig. S36 Self-healing of an actuator constructed from **P_{53}(5)** 6.7 V/μm at 0.25 Hz.

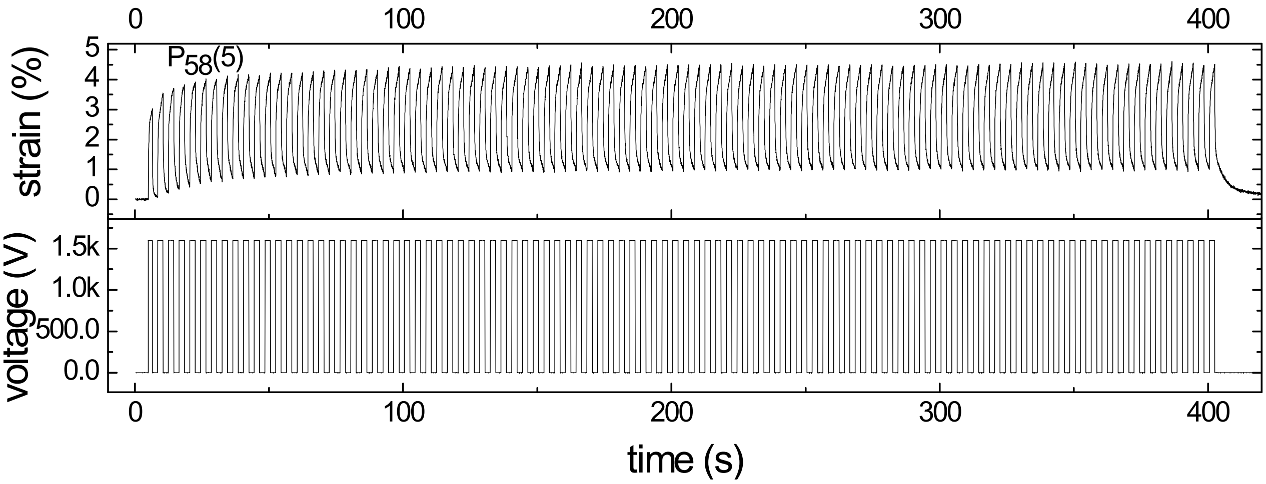

Fig. S37 Long-term stability of $\mathbf{P_{58}(5)}$ at 10.2 V/μm for 100 cycles at 0.25 Hz.